# Sensorless Stator Turn-to-Turn Fault Detection in Induction Machine based on MRAS Observer: Experimental Validations

**M A. HAMIDA**
Ouargla University, Faculty of New Technology of Information and communication
01 avenue de 1er Novembre, 30000 Ouargla, Algérie, mohamedassaad.hamida@univ-ouargla.dz

**S. MOREAU**
University of Poitiers, LIAS-ENSIP
2 rue Pierre Brousse, BP 633, 86022 Poitiers Cedex, France, sandrine.moreau@univ-poitiers.fr

***Abstract:*** *In this paper the problem of stator turn-to-turn fault detection is studied. The proposed technique is based on the residual generates from the error between the faulty system state and the reference one. A model reference adaptive system (MRAS) observer is designed in order to estimate the induction machine states and to detect stator turn-to-turn faults.*
*A special three-phase induction machine has been constructed in order to simulate real faulty experiments. Simulation and experimental results show the effectiveness of the proposed strategy.*

***Key words:*** *Stator fault detection, Induction machine, MRAS observer, Sensorless control.*

**Nomenclature**

| | |
|---|---|
| $I_{sd}$, $I_{sq}$ | stator $d$ and q axis currents |
| $V_{sd}$, $V_{sq}$ | stator $d$ and $q$ axis voltages |
| $\Phi_{rd}$, $\Phi_{rq}$ | rotor $d$ and $q$ axis fluxes |
| $L_f$ | global-linkage inductance |
| $L_m$ | mutual inductance |
| $R_s$ | stator resistance |
| $R_r$ | rotor resistance |
| $K_{p\_id}$, $K_{i\_id}$ | integral and proportional (IP) current controller |
| $K_{p\_iq}$, $K_{i\_iq}$ | integral and proportional (IP) current controller |
| $K_{p\_\omega}$, $K_{i\_\omega}$ | integral and proportional (IP) speed controller |
| J | total rotor inertia |
| F | viscous friction coefficient |
| $T_e$ | electromagnetic torque |
| $T_l$ | load torque |

## 1. Introduction.

Speed controlled Induction Machines (IM) are widely exploited in several industrial fields thanks to their robustness and limited cost [1]. Control algorithms for inductions motors used in high performances applications require feedback information of rotor position and, for speed tracking applications, of rotor speed. As a consequence, so-called "*sensorless*" control methods [2-5] attracted the industrial interest [6] to avoid the use of mechanical sensors and has induced an intensive research activity in the control community of different types of electrical machines, such as induction machines, stepper motors, PMSM. The approaches mentioned above share a common method consisting in building one or several observers based on the use of the electrical variables of Induction Machines [7,8] for example. Nonetheless, the electrical variables may also undergo faults affecting the IM normal functioning, with serious consequences on the effectiveness of eventual sensorless control techniques [9].

Fault detection is becoming more and more important for variable speed drives to increase availability and reliability and reduce downtime [10].

Recently, several methods were applied for fault detection and isolation purpose of electrical machines, among which analytical redundancy relations [11, 12, 13], parity equations or observers [14], [15], [16], [17] can be cited.

To solve estimation and residual generation problems, several techniques have been proposed in the literature, such as Kalman filter [18], high gain observer [19], sliding mode observer [20], unknown inputs observer [21] and Integral Proportional observer [22]. All these techniques are based on model-based fault diagnosis and residual generation.

By comparing the methods developed previously in the literature, we found that the model reference adaptive system (MRAS) technique is one of the best methods to estimate the rotor speed and for the diagnosis of induction machine [23]. This technique

is preferred thanks to its simplicity, its easy implementation, and its proven stability [24].

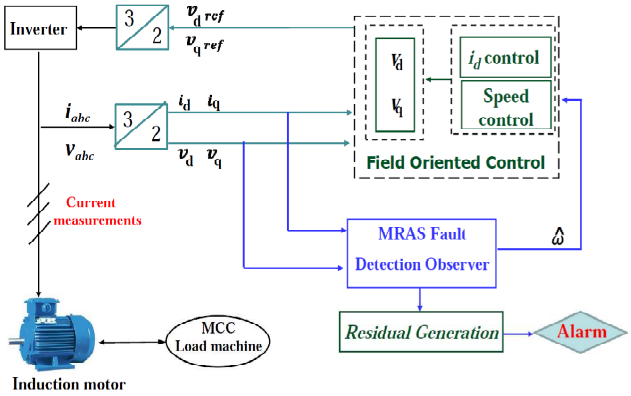


Fig. 1. Overview of the considered IM fault detection strategy.

This paper presents a model-based residual generation procedure for a rotor field oriented control of IM (Fig.1).The gains of the Integral Proportional (IP) currents and speed controllers are given in Appendix A. It proposes also a robust sensorless MRAS observer, which is applied to diagnose electrical faults of an induction motor, such as stator short circuits. The short-circuit fault can be detected by analyzing the residual between measured and observed variables. The proposed diagnosis strategy is tested through several simulations and experiments.

The paper is organized as follows: the healthy mathematical model of the Induction Machine is introduced in Section (2). This model is used for the IM controller and the MRAS observer. Then, in order to simulate stator short-circuit faults of the IM, its faulty model is recalled in section (3). Section (4) is devoted to fault detection and estimation with the introduction of the MRAS observer. Section (5) contains the simulation of the proposed strategy. Finally, in Section (6), the proposed diagnosis strategy is tested experimentally.

## 2. Induction machine healthy model

Under standard hypotheses (linear magnetic circuits, balanced operating conditions, negligible iron losses and effects of end windings and slots), the equivalent two-phase electro-magnetic model of the three-phase Induction Machine, expressed in a Park's reference frame (d, q) linked to the rotor, is given by [25]

$$\begin{cases} [\dot{X}] = [A(\omega)].[X] + [B] \\ [Y] = [C].[X] \end{cases} \quad (1)$$

$$J\frac{d}{dt}(\Omega) = Te - T_l - F\Omega \quad (2)$$

Where:

$$[X] = \begin{bmatrix} I_{sd} \\ I_{sq} \\ \Phi_{rd} \\ \Phi_{rq} \end{bmatrix}; \quad [B] = \begin{bmatrix} \frac{1}{L_f} & 0 \\ 0 & \frac{1}{L_f} \\ 0 & 0 \\ 0 & 0 \end{bmatrix};$$

$$A = \begin{bmatrix} -\left(\frac{R_s + R_r}{L_f}\right) & 0 & \frac{R_r}{L_m L_f} & \frac{\omega}{L_f} \\ 0 & -\left(\frac{R_s + R_r}{L_f}\right) & -\frac{\omega}{L_f} & \frac{R_r}{L_m L_f} \\ R_r & 0 & -\frac{R_r}{L_m} & -\omega \\ 0 & R_r & \omega & -\frac{R_r}{L_m} \end{bmatrix}$$

$$[U] = \begin{bmatrix} V_{sd} \\ V_{sq} \end{bmatrix}; \; [C] = \begin{bmatrix} 1 & 0 & 0 & 0 \\ 0 & 1 & 0 & 0 \end{bmatrix}; \; [Y] = \begin{bmatrix} I_{sd} \\ I_{sq} \end{bmatrix};$$

## 3. Induction machine faulty model

In order to take into account the presence of inter-turn short-circuit windings in the stator of an induction motor, an original stator faulty model was proposed in [26]. In faulty case, an induction machine can be characterized by two equivalent modes: the common mode model which corresponds to the healthy dynamics of the machine (Park's model) and the differential mode model which explains the faults. This stator faulty model is used for the present study. It is established in dq Park's reference frame with global leakages referred to the stator and it is composed of three short circuit dipoles $Q_{cci}$ added in parallel to explain a stator short circuit fault on each phase (Fig. 2). For example, a short-circuit winding on phase b will induce in stator a new short circuited winding *Bcc* localized according to the first phase a by the angle $\theta cc = 2\pi/3$ rad.

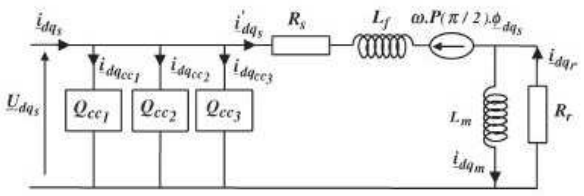


Fig 2: Stator short-circuit model of three phase Induction Machine.

We consider the following state space representation:

$$\begin{cases} \dot{x} = Ax(t) + Bu(t) \\ y(t) = Cx(t) + Du(t) \end{cases} \quad (3)$$

Where D represents the anticipation matrix, given by:

$$D = \sum_{k=1}^{3} \frac{2\eta_{cck}}{3R_s} Q(\theta_{cck}) \quad (4)$$

The short-circuit report $\eta_{cc}$ is the ratio of the number of turns in short circuit on the total number of coils in a stator phase without default. This parameter quantifies the fault severity and gives the number of turns in short circuit.

$$\eta_{cck} = \frac{n_{cck}}{n_s} \quad (5)$$

$n_{cck}$ : Number of inter-turn short-circuit windings on phase $k$.

$n_s$ : Total number of inter-turn in healthy phase.

$$i_{dqs} = i'_{dqs} + \sum_{k=1}^{3} i_{dqcck} \quad (6)$$

$i_{dqcck}$: short-circuit current of phase $k$.

The matrix $Q_{cck}(\theta_{cck})$ allows the fault localization via the angle $\theta_{cck}$ ($\theta_{cck} = 0$ for the phase a).

$$Q_{cck}(\theta_{cck}) = \begin{pmatrix} \cos(\theta_{cck})^2 & \cos(\theta_{cck})\sin(\theta_{cck}) \\ \cos(\theta_{cck})\sin(\theta_{cck}) & \sin(\theta_{cck})^2 \end{pmatrix} \quad (7)$$

## 4. MRAS observer

The method of MRAS (Model Reference Adaptive System) is based on the choice of two models to represent a system. The first one is called "reference model" and the other one is named "adaptive model". MRAS is used to design the adaptive PI controller that works on the principle of adjusting the controller parameters so that the output of the adaptive model tracks the output of a reference model having the same reference input. The MRAS estimator is designed here to estimate the stator currents, the rotor flux and the rotor speed.

The main idea behind MRAS method is that there is a reference model and an adjustable one. The first model is used to determine the required states and the second one is an adaptive model, which provides the estimated values of the states [27]. The output of the reference model is compared with an adjustable observer-based model. The error obtained between the reference and the adjustable model is given to an adaptation mechanism, which adjusts the adaptive model by generating the estimated value of rotor speed. The block diagram of the estimation technique based on MRAS method is shown in Figure 3.

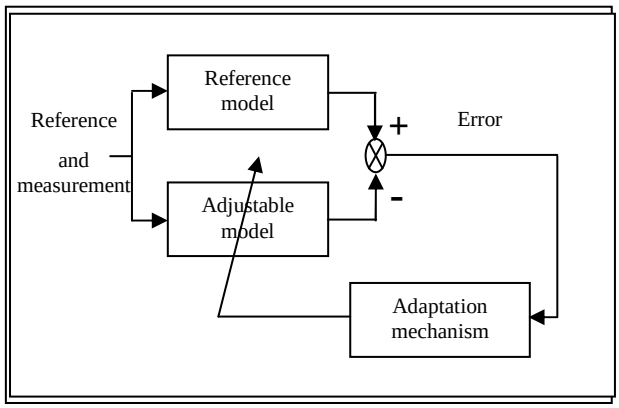


Fig. 3. Block diagram of the estimation technique with MRAS observer.

From (1), the reference state space model of the Induction Machine in α−β reference frame is given by:

$$\begin{cases} [\dot{X}] = [A(\omega)].[X] + [B].[U] \\ [Y] = [C].[X] \end{cases} \quad (8)$$

Where:

$$[X] = \begin{bmatrix} I_{sd} \\ I_{sq} \\ \Phi_{rd} \\ \Phi_{rq} \end{bmatrix}; \quad [U] = \begin{bmatrix} V_{sd} \\ V_{sq} \end{bmatrix}; \; [Y] = \begin{bmatrix} I_{sd} \\ I_{sq} \end{bmatrix}$$

with:

$$A = \begin{bmatrix} \begin{bmatrix} a_1 & 0 \\ 0 & a_1 \end{bmatrix} & \begin{bmatrix} a_2 a_4 & a_2\widehat{\omega} \\ a_2\widehat{\omega} & a_2 a_4 \end{bmatrix} \\ \begin{bmatrix} a_3 & 0 \\ 0 & a_3 \end{bmatrix} & \begin{bmatrix} a_4 & -\widehat{\omega} \\ \widehat{\omega} & a_4 \end{bmatrix} \end{bmatrix};$$

$$[B] = \begin{bmatrix} b & 0 \\ 0 & b \\ 0 & 0 \\ 0 & 0 \end{bmatrix}; \; [C] = \begin{bmatrix} 1 & 0 & 0 & 0 \\ 0 & 1 & 0 & 0 \end{bmatrix}.$$

And: $a_1 = -\frac{R_s + R_r}{L_f}$ ; $a_2 = \frac{1}{L_f}$ ; $a_3 = R_r$ ; $a_4 = \frac{R_r}{L_r}$ ; $b = \frac{1}{L_f}$.

A Luenberger observer for the Induction Machine

system (7) is given by:

$$\begin{cases}\dot{\hat{X}} = A(\omega).\hat{X} + B.U + K\varepsilon_Y \\ \hat{Y} = C.\hat{X}\end{cases} \quad (9)$$

Its gain can be computed as:

$$A(\omega) = \begin{bmatrix} a_1 & 0 & a_2 a_4 & a_2\hat{\omega} \\ 0 & a_1 & a_2\hat{\omega} & a_2 a_4 \\ a_3 & 0 & a_4 & -\hat{\omega} \\ 0 & a_3 & \hat{\omega} & a_4 \end{bmatrix} \quad (10)$$

(8) can be represented as follows:

$$\dot{\hat{X}} = A(\omega).\hat{X} + B.U + K(I_s - \hat{I}_s) \quad (11)$$

With:

$$K = \begin{bmatrix} k_1 & -k_2\hat{\omega} \\ k_2\hat{\omega} & k_1 \\ k_3 & -k_4\hat{\omega} \\ k_4\hat{\omega} & k_3 \end{bmatrix}, (I_s - \hat{I}_s) = \begin{bmatrix} I_{sd} - \hat{I}_{sd} \\ I_{sq} - \hat{I}_{sq} \end{bmatrix}$$

$$\dot{e} = (A - KC)e + (\Delta A)\hat{X} \quad (12)$$

With :

$$\Delta A = A(\omega) - A(\hat{\omega}) = \begin{bmatrix} 0 & 0 & 0 & a_2 p\Delta\omega \\ 0 & 0 & a_2 p\Delta\omega & 0 \\ 0 & 0 & 0 & -p\Delta\omega \\ 0 & 0 & p\Delta\omega & 0 \end{bmatrix} \quad (13)$$

The value of the rotor speed error is given as:

$$\Delta\omega = \omega - \hat{\omega} \quad (14)$$

The difference between the state model given by Eq. (7) and the adjustable model given by Eq. (10) is used to drive a suitable adaptation mechanism.

This difference is expressed by:

$$e = X - \hat{X} = \begin{bmatrix} e_{I_{sd}} \\ e_{I_{sq}} \\ e_{\Phi_{rd}} \\ e_{\Phi_{rq}} \end{bmatrix} \quad (15)$$

Now, we define the following Lyapunov function:

$$V = e^T e + \Delta\omega^2/\lambda \quad (16)$$

Its derivative with respect to time is:

$$\frac{dV}{dt} = \left\{\frac{d(e^T)}{dt}\right\} e + e^T \left\{\frac{de}{dt}\right\} + \frac{1}{\lambda}\frac{d}{dt}(\Delta\omega^2)$$

(17)

This derivative can be detailed by the following equation:

$$\frac{dV}{dt} = e^T\{(A - KC)^T + (A - KC)\}e -$$

$$2a_2\Delta\omega\left(e_{I_{sd}}\hat{\Phi}_{rq} - e_{I_{sq}}\hat{\Phi}_{rd}\right) + \frac{2}{\lambda}\Delta\omega\frac{d}{dt}\Delta\omega^2 \quad (18)$$

From this equation, we can deduce the following adaptation law to estimate the rotor speed:

$$\hat{\omega} = \lambda.a_2\int_0^t\left(e_{I_{sd}}\hat{\Phi}_{rq} - e_{I_{sq}}\hat{\Phi}_{rd}\right)dt \quad (19)$$

Where $\lambda$ is a positive constant.

However, this adaptation law is established for a constant speed and to improve the response of the adaptation algorithm. The speed estimated by a PI controller is given by the following relationship

$$\hat{\omega} = k_p\left(e_{I_{sd}}\hat{\Phi}_{rq} - e_{I_{sq}}\hat{\Phi}_{rd}\right) + k_i\int\left(e_{I_{sd}}\hat{\Phi}_{rq} - e_{I_{sq}}\hat{\Phi}_{rd}\right)dt \quad (20)$$

Where $k_p$ and $k_i$ are positive adaptation gains of the PI observer.

A PI controller is sufficient to guarantee the stability of the system.

## 5. Simulation results

This section presents simulation results obtained from sensorless speed control of Induction Machine. The simulation was performed with the Matlab–Simulink software environment using the motor parameters listed in Table 1. The speed loop and the current $i_d$ control are realized by integral proportional (IP) controllers.

Table 1
Induction Machine parameters

| | |
|---|---|
| Rs | 11 Ω |
| Rr | 3.62 Ω |
| Lf | 60 mH |
| Lm | 420 mH |
| J | 0.04 kg m$^2$ |
| p (poles pair number) | 2 |
| Tl | 7 Nm |

The Figures 4 to 12 show the simulation results of the sensorless fault detection control of the Induction Machine. The machine parameters are the same as the parameters used for the MRAS observer.

Figure 4 shows the measured speed with the observed one. In this figure it can be clearly seen that the observed speed tracks very well the measured one.

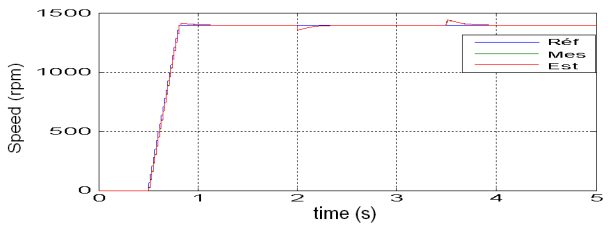


Fig. 4. Observed speed & Measured speed in the healthy case with applied load torque (from 2s to 3.5s).

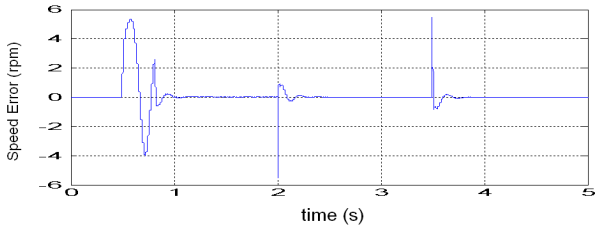


Fig. 5. Observation error less than 0.5% despite applied load torque.

For this case, we can clearly see the efficiency of the proposed sensorless control under load torque (see the small observation error given by the Figure 5).

Figure 6 shows the sensorless operation at very low speed in the two rotation senses.

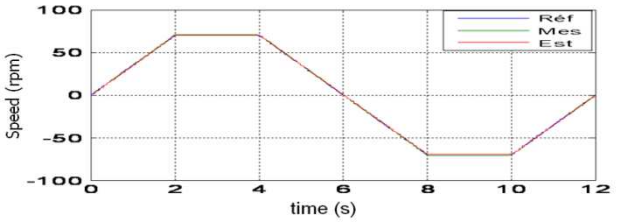


Fig. 6. Observed speed and measured speed at very low speed operation.

The zone at very low speed is very critical for sensorless operation. Figure 7 shows the high performance of the proposed strategy in this zone.

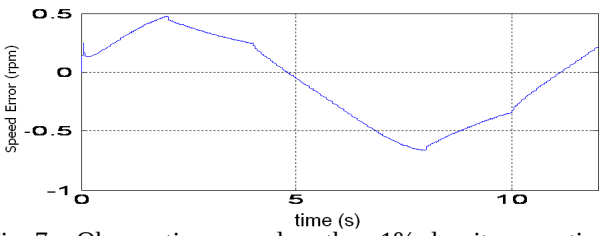


Fig. 7. Observation error less than 1% despite operation at very low speed.

The average value of the rotor speed error converges to zero, as shown in Figure 7.

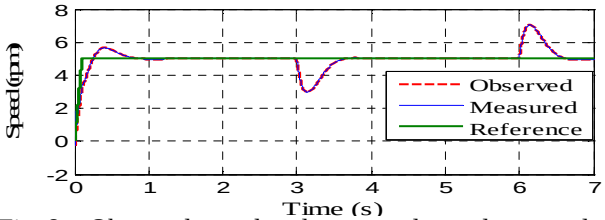


Fig. 8. Observed speed and measured speed at very low speed operation with full load torque.

Figure 8 shows the sensorless operation at very low speed with full load torque applied between 3 and 6 second. This figure illustrates the good performance of the proposed sensorless strategy in critical operation area.

Now, the performance and the effectiveness of the proposed sensorless fault detection strategy are tested by computer simulation. The simulation results show the response for a stator short-circuit of 58 coils. The short-circuit is applied to one phase from t=3s to t=5s.

Although the speed follows its control trajectory (see Figure 9), a variation is noticed on the observed speed signal (see Figure 9 at t=3s). This variation is due to the introduction of the stator short-circuit.

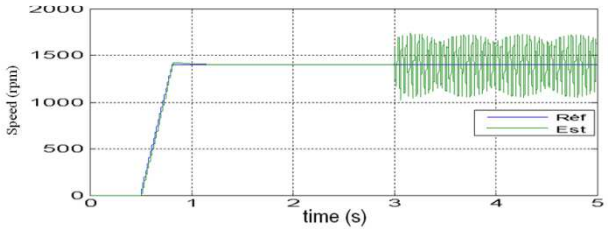


Fig. 9. Rotor speed with short-circuit fault activated from t=3s.

The speed residual generated from the difference between the measured speed and the observed one is shown in the Figure 10. In Figure 11, the difference between the estimated and the measured stator currents indicates also the occurrence of a fault.

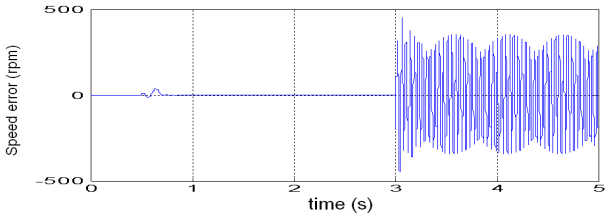


Fig. 10. Rotor speed residual of the short-circuit fault activated from t=3s.

So the short-circuit fault can also be detected by analyzing the current signals. Before introducing the short-circuit fault, we can see that the observed current tracks very well the measured one. But the

stator short-circuit introduced at t=3s disrupts the observation from t=3s.

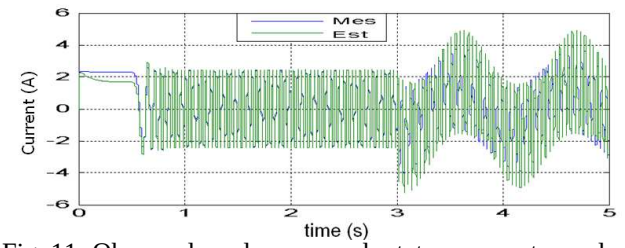


Fig. 11. Observed and measured stator currents under short-circuit fault activated at t=3s.

The residual generated from the difference of the observed current and the measured one (observation error) shown by Figure 12 indicates the occurrence of a fault.

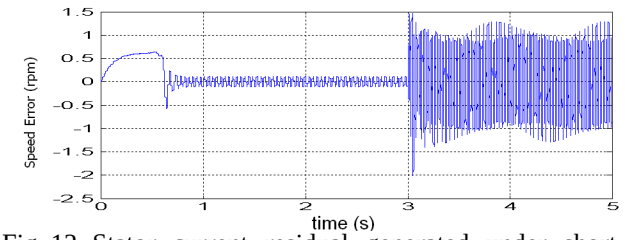


Fig. 12. Stator current residual generated under short-circuit fault activated at t=3s.

Consequently, the simulation results show the efficiency and the feasibility of the proposed sensorless fault detection strategy of Induction Machine based on MRAS scheme. This work is validated experimentally using a special rewound Induction Machine. The experimental results are shown in the next section.

## 6. Experimental results

The effectiveness and the performances of the proposed sensorless control and fault detection strategy of the Induction Machine were experimentally tested following the controller-observer scheme given in Figure 1.

dSPACE DS1104 controller board was used to implement the control and detection fault algorithms in real-time. The parameters of the motor are listed in Table 1. The coding of real-time control software was done using C language. The sampling period was set to 0.1 ms. The IM is fed by a three phase IGBT inverter supplied by a DC link voltage of 410V. The PWM frequency is set to 12 kHz. The Pulse Width Modulated (PWM) signals [28] were generated by the DS1104 board [29].
An incremental encoder was used to obtain the measured position signal solely used for comparison.

The developed test bench (shown in Figure 13) is located at LIAS laboratory in Poitiers University, France.

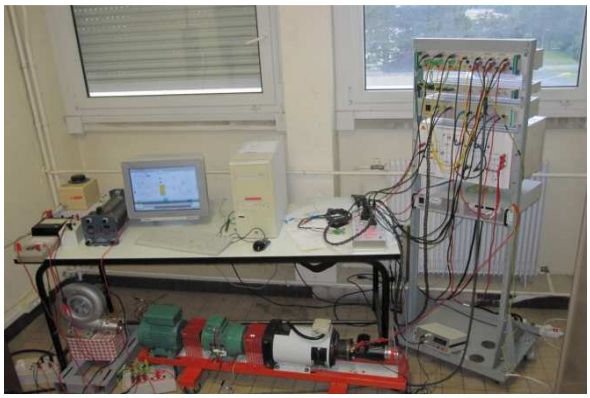

Fig. 13. Experimental test bench located at LIAS ENSIP France.

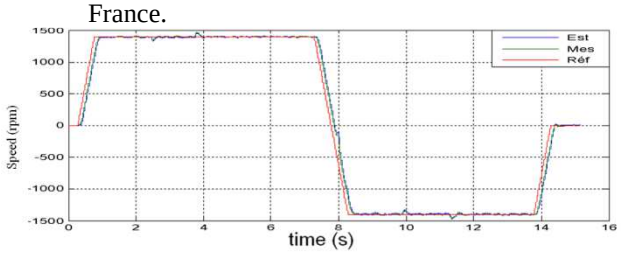


Fig. 14. Observed and Measured speed in the healthy case with applied load torque (from 2.5s to 4s and from 10s to 11.5s).

The Figures 14 to 17 give the experimental results of sensorless control fault detection for Induction Machine. The controller and the observer are designed by using the nominal IM parameters in healthy case (given in Table 1).
Figure 14 shows the observed speed with the measured one. We can observe that the estimated speed tracks the measured one very well. The speed error due to load torque disturbance introduced from 2.5s to 4s and from 10s to 11.5s is very small. This figure shows also the machine operation in the two rotation senses, that confirms the effectiveness of the proposed observer.

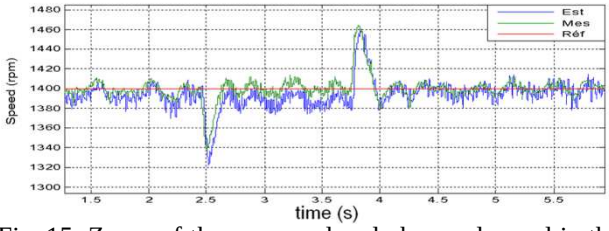


Fig. 15. Zoom of the measured and observed speed in the nominal case.

Figure 15 shows a zoom of the measured speed and the observed one at nominal speed with a load torque applied from 2.5s to 4s. We can see that the estimated rotor speed accurately follows the reference one, even at stand-still speed operation. So

this figure shows the robustness of the proposed strategy.

To evaluate the effectiveness of the proposed observer for fault detection, a short-circuit of 58 coils was introduced on one phase of stator windings. The short-circuit is introduced from 6s to 8,5s. On Figure 16, we can clearly see the influence of the introduced fault on the observed speed.

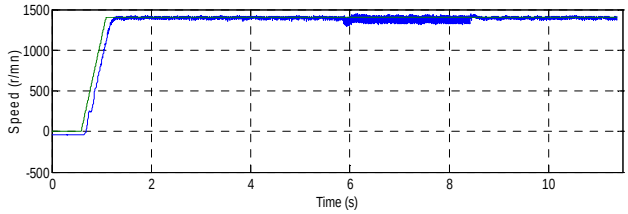


Fig. 16. Rotor speed with short-circuit fault activated between 6s and 8,5s.

The residual generated by the observer is given by Figure 17. We can see that the residual value is more important from 6s to 8.5s, which allows to detect the short-circuit fault.

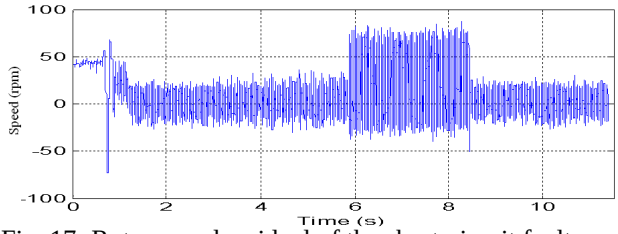


Fig. 17. Rotor speed residual of the short-circuit fault activated between 6s and 8.5s.

## 7. Conclusion

The early bird fault detection is able to prevent catastrophic faults. The problem of the Induction Machine sensorless fault detection is studied in this paper. To detect short-circuit faults of the induction machine, a MRAS observer is developed and investigated by simulations and experiments. The obtained results in simulation and experimentally show the effectiveness and the performances of the proposed strategy. These results show that a clear fault indicator can be defined by the residuals generated from the difference between the observed states and the measured ones.

In this study, only stator short-circuits were considered. The proposed methodology will be applied to broken rotor bars detection in future work.

### References


1. Sudhoff, S.D, Aliprantis, D.C, Kuhn, B.T, Chapman, P.L "An induction machine model for predicting inverter-machine interaction," , IEEE Transactions on Energy Conversion , vol.17, no.2, pp.203,210, Jun 2002.
2. Yamamoto, S, Hirahara, H.; Tanaka, A.; Ara, T.; Matsuse, K., "Universal Sensorless Vector Control of Induction and Permanent-Magnet Synchronous Motors Considering Equivalent Iron Loss Resistance," Industry Applications, IEEE Transactions, vol. 51, n°2, pp.1259,1267, March-April 2015.
3. Stojic, D.; Milinkovic, M.; Veinovic, S.; Klasnic, I., "Improved Stator Flux Estimator for Speed Sensorless Induction Motor Drives," Power Electronics, IEEE Transactions, vol. 30, n° 4, pp.2363,2371, April 2015.
4. N. Bensiali, E. Etien, N. Benalia, Convergence analysis of back-EMF MRAS observers used in sensorless control of induction motor drives, Mathematics and Computers in Simulation, Volume 115, September 2015, Pages 12-23, ISSN 0378-4754.
5. Lihang Zhao, Jin Huang; He Liu, Bingnan Li, Wubin Kong, "Second-Order Sliding-Mode Observer With Online Parameter Identification for Sensorless Induction Motor Drives," Industrial Electronics, IEEE Transactions on , vol.61, no.10, pp.5280,5289, Oct. 2014.
6. Anno Yoo, Chanook Hong, Young-Doo Yoon, "Sensorless torque control of induction machine in low speed and low torque region," Power Electronics and Applications (EPE'14-ECCE Europe), 2014 16th European Conference on , vol., no., pp.1,8, 26-28 Aug. 2014.
7. Raute, R, Caruana, C, Staines, C.S, Cilia, J, Sumner, M, Asher, G, "Sensorless Control of Induction Machines by Using PWM Harmonics for Rotor Bar Slotting Detection," *Industry Applications Society Annual Meeting, 2008. IAS '08. IEEE* , vol., no., pp.1,8, 5-9 Oct. 2008.
8. K. Negadi, A. Mansouri, B. Khatemi, "Real Time Implementation Of MRAS and design Kalman Filter Based Speed Sensorless Vector Control Of Induction Motor, Journal of Electrical engineering, vol.8,2008.

   Caruso, M.; Cecconi, V.; Di Tommaso, A.O.; Rocha, R., "Sensorless variable speed single-phase induction motor drive system," *Industrial Technology (ICIT), 2012 IEEE International Conference on* , vol., no., pp.731,736, 19-21 March 2012.
9. Chakraborty, C.; Verma, V., "Speed and Current Sensor Fault Detection and Isolation Technique for Induction Motor Drive Using Axes Transformation," *Industrial Electronics, IEEE Transactions on* , vol.62, no.3, pp.1943,1954, March 2015.
10. Diallo, D.; Benbouzid, M.E.H.; Hamad, D.; Pierre, X., "Fault Detection and Diagnosis in an Induction Machine Drive: A Pattern Recognition Approach Based on Concordia Stator Mean Current Vector," *Energy Conversion, IEEE Transactions on* , vol.20, no.3, pp.512,519, Sept. 2005.
11. Seshadrinath, J.; Singh, B.; Panigrahi, B.K., "Incipient Interturn Fault Diagnosis in Induction Machines Using an Analytic Wavelet-Based Optimized Bayesian Inference," *Neural Networks and Learning Systems, IEEE Transactions on* , vol.25, no.5, pp.990,1001, May 2014.

12. Yong-Hwa Kim; Young-Woo Youn; Don-Ha Hwang; Jong-Ho Sun; Dong-Sik Kang, "High-Resolution Parameter Estimation Method to Identify Broken Rotor Bar Faults in Induction Motors,"*Industrial Electronics, IEEE Transactions on* , vol.60, no.9, pp.4103,4117, Sept. 2013.
13. Rothenhagen, K.; Fuchs, F.W., "Doubly Fed Induction Generator Model-Based Sensor Fault Detection and Control Loop Reconfiguration," *Industrial Electronics, IEEE Transactions on* , vol.56, no.10, pp.4229,4238, Oct. 2009.
14. Kallesoe, C.S.; Cocquempot, V.; Izadi-Zamanabadi, R., "Model based fault detection in a centrifugal pump application," *Control Systems Technology, IEEE Transactions on* , vol.14, no.2, pp.204,215, March 2006.
15. Xinan Zhang; Foo, G.; Don Vilathgamuwa, M.; Tseng, K.J.; Bhangu, B.S.; Gajanayake, C., "Sensor fault detection, isolation and system reconfiguration based on extended Kalman filter for induction motor drives," *Electric Power Applications, IET* , vol.7, no.7, pp.607,617, Aug. 2013.
16. Morawiec, M., "Z-Type Observer Backstepping for Induction Machines," Industrial Electronics, IEEE Transactions on , vol.62, no.4, pp.2090,2102, April 2015.
17. Alonge, F.; Cangemi, T.; D'Ippolito, F.; Fagiolini, A.; Sferlazza, A., "Convergence Analysis of Extended Kalman Filter for Sensorless Control of Induction Motor," Industrial Electronics, IEEE Transactions on , vol.62, no.4, pp.2341,2352, April 2015.
18. Mahamoud, A.; Glumineau, A.; Souleiman, I., "On a new strategy for induction motors fault detection and isolation," Control and Automation (ICCA), 2010 8th IEEE International Conference on , vol., no., pp.1428,1433, 9-11 June 2010.
19. Kommuri, S.K.; Rath, J.J.; Veluvolu, K.C.; Defoort, M., "An induction motor sensor fault detection and isolation based on higher order sliding mode decoupled current controller," Control Conference (ECC), 2014 European , vol., no., pp.2945,2950, 24-27 June 2014.
20. Ghazal, M.; Poshtan, J., "Robust stator winding fault detection in induction motors," Power Electronics, Drive Systems and Technologies Conference (PEDSTC), 2011 2nd , vol., no., pp.163,168, 16-17 Feb. 2011.
21. D.R. Espinoza-Trejo, D.U. Campos-Delgado,E. Bárcenas, F.J. Martínez-López, "Robust fault diagnosis scheme for open-circuit faults in voltage source inverters feeding induction motors by using non-linear proportional-integral observers", IET Power Electronics, Volume 5, Issue 7, pp. 1204 – 1216, August 2012.
22. S. Maiti, C. Chakraborty, S. Sengupta, Simulation studies on model reference adaptive controller based speed estimation technique for the vector controlledpermanent magnet synchronous motor drive, Simulation Modelling Practiceand Theory 17 (4) (2009) 585–596.
23. C. Schauder, "Adaptive speed identification for vector control of induction motors without rotational transducers," IEEE Trans. Ind. Applicat., vol. 28, pp. 1054–1061, Sept./Oct. 1992.
24. Rogers, G.J.; Shirmohammadi, D., "Induction Machine Modelling for Electromagnetic Transient Program," IEEE Power Engineering Review , vol. 7, no.12, pp.37,38, Dec. 1987.
25. Joksimovic, G.M.; Penman, J., "The detection of inter-turn short circuits in the stator windings of operating motors," *Industrial Electronics, IEEE Transactions on* , vol.47, no.5, pp.1078,1084, Oct 2000.
26. Bachir, S.; Tnani, S.; Trigeassou, J.-C.; Champenois, G., "Diagnosis by parameter estimation of stator and rotor faults occurring in induction machines," *Industrial Electronics, IEEE Transactions on* , vol.53, no.3, pp.963,973, June 2006.
27. Cirrincione, M.; Accetta, A.; Pucci, M.; Vitale, G., "MRAS Speed Observer for High-Performance Linear Induction Motor Drives Based on Linear Neural Networks," *Power Electronics, IEEE Transactions on* , vol.28, no.1, pp.123,134, Jan. 2013.
28. Agarwal, A.; Agarwal, V., "FPGA Realization of Trapezoidal PWM for Generalized Frequency Converter," IEEE Transactions on Industrial Informatics, vol.8, no.3, pp.501,510, Aug. 2012.
29. Al Nabulsi, A.; Dhaouadi, R., "Efficiency Optimization of a DSP-Based Standalone PV System Using Fuzzy Logic and Dual-MPPT Control," IEEE Transactions on Industrial Informatics, vol.8, no.3, pp.573-584, Aug. 2012.

**Appendix A.**

**Controllers parameters of the rotor field oriented vector control of the Induction Machine:**

The Integral and Proportional (IP) controllers on d and q-axis currents (not detailed here) are tuned with the following parameters:

$K_{p\_id}= 87$ [p.u] and $K_{i\_id}= 315$ [s], $K_{p\_iq}= 101$ [p.u] and $K_{i\_iq}= 325$ [s]

The parameters of the speed Integral Proportional (IP) controller are set to:

$K_{p\_\omega}= 12$ [p.u] and $K_{i\_\omega}= 25$ [s]